Amino Acids (2014) 46:209–222
DOI 10.1007/s00726-013-1620-z

ORIGINAL ARTICLE

BP5 regulated B cell development promoting anti-oxidant defence

Xiao-Dong Liu · Bin Zhou · Rui-Bing Cao · Xiu-Li Feng · Zhi-Yong Ma · Pu-Yan Chen

Received: 28 July 2013 / Accepted: 3 November 2013 / Published online: 29 November 2013

Abstract Bursa of Fabricius is the humoral immune system for B cell differentiation and antibody production. Bursopentine (BP5) is a novel immunomodulatory peptide and significantly stimulated an antigen-specific immune response in mice. BP5 was also found to protect LPS-activated murine peritoneal macrophages from oxidative stress. In this study, the effects of BP5 on B cell development were examined. The results suggested that BP5 markedly promoted B cell development by increasing CFU-pre B, and affected the redox homeostasis regulation of B cells. To study the molecular mechanism of effect of bursal-derived BP5, this research utilized 2D-E and MALDI-TOF/TOF to analyze the differentially expressed proteins of BP5-treated WEHI-231 cells. The results showed that BP5 affected the redox homeostasis regulation of WEHI-231 cells and induced alterations in the protein expression profiles related to the oxidoreduction coenzyme metabolic process, precursor metabolites and energy, proteolysis, RNA splicing and translation and cellular process, respectively. BP5 also induced glucose-6-phosphate dehydrogenase (G6PD) activity, an essential anti-oxidant cofactor. We found that the redox homeostasis regulation effect of BP5 was reduced in G6PD-deficient cells. These data suggested that BP5 affected the redox balance toward reducing conditions by promoting the expression of G6PD, which in turn regulated the glutathione redox cycle and other processes.

Keywords BP5 · ROS · Two-dimensional gel electrophoresis · G6PD

Abbreviations

BF	The bursa of Fabricius
ROS	Reactive Oxygen Species
MALDI-TOF/TOF	Matrix-assisted laser desorption/ ionization-time of flight mass spectrometry
2D-E	Two-dimensional gel electrophoresis
DTT	Dithiothreitol
CHAPS	3-[(3-Cholamidopropyl) dimethylammonio] propanesulfonate
FITC	Fluorescein isothiocyanate
PPP	Pentose phosphate pathway

Introduction

The bursa of Fabricius (BF), a primary humoral immune organ unique to birds (Davison et al. 2008), is critical for B-lymphocyte differentiation (Cooper et al. 1966; Glick et al. 1956; Lydyard et al. 1976). In mammals, the B cell-differentiating organ which is equivalent to the T-cell-differentiating thymus has not been defined (Brand et al. 1976). Therefore, BF provides an invaluable model for studies on basic immunology.

Several small peptides have been used in clinical applications. Thymopentin has been used in treating

X.-D. Liu · B. Zhou · R.-B. Cao · X.-L. Feng · P.-Y. Chen (✉)
Division of Key Laboratory of Animal Disease Diagnosis and Immunology of China's Department of Agriculture, Nanjing Agricultural University, Nanjing 210095, People's Republic of China
e-mail: 2010207012@njau.edu.cn; puyanchen@yahoo.com.cn

Z.-Y. Ma
Chinese Academy of Agricultural Science, Shanghai Veterinary Research Institute, No. 518, Ziyue Road, Shanghai 200241, People's Republic of China

various diseases (Singh et al. 1998), and cancer (Sundal 1992). Glutathione, (GSH) a well-known tripeptide (Glu-Cys-Gly) has immune-stimulating and antioxidant activities (Dröge and Breitkreutz 2000). It has been reported that BF also contains some biological active factors. For example, Bursin, as a candidate specific molecule for the differentiation of B cells (Lassila et al. 1989), selectively stimulates avian B cells, but not avian T cells, from their precursors in vitro (Audhya et al. 1986), and promotes immunoglobulin switching from IgM to IgG (Baba and Kita 1977). Bursal Anti-Steroidogenic Peptide (BASP) is responsible for synchronization of B-cell division during embryogenesis and neonatal life (Moore and Caldwell 2003). Therefore, bursal bioactive peptides exert various functions during B cell development and humoral immunity response. Several other small peptides have been used in clinical applications. Thymopentin has been used in treating various diseases (Singh et al. 1998), and cancer (Sundal 1992). GSH, a well-known tripeptide (Glu-Cys-Gly) has immune-stimulating and antioxidant activities (Dröge and Breitkreutz 2000).

In our recent study, a new BF isolated biological active factor Bursopentine (BP5) was proved to be a multifunctional modulator in immune response (Li et al. 2011). A number of hemopoietic cells, including dendritic cells (DCs) (Angelini et al. 2002), activated B cells (Castellani et al. 2008), and monocytes (Tassi et al. 2009) have been reported to generate low-molecular-weight thiols in vitro. BP5 is a new thiol-containing pentapeptide, contains a cysteine in the N-terminal, could protect LPS-activated murine peritoneal macrophages from oxidative stress (Li et al. 2011). In this paper, the effects of BP5 and its underlying molecular mechanism were examined in WEHI-231 cells through proteomics analysis. Results from these analyses showed that BP5 markedly promoted B cell development by increasing CFU-pre B, and affected the redox balance toward reducing conditions of B cells. BP5 also up-regulated the anti-oxidant systems of WEHI-231 B cells through regulating expression of glucose-6-phosphate dehydrogenase (G6PD), which in turn regulated the GSH redox cycle and various cellular processes, including oxidoreduction coenzyme metabolic process, precursor metabolites and energy, proteolysis, RNA splicing and translation and cellular process.

Materials and methods

Cell line and animals

WEHI 231 cells were maintained in RPMI 1640 medium (Gibco) supplemented with 10 % fetal bovine serum (FBS) (HyClone Laboratories, Logan, UT, USA), 1,250 U/ml penicillin G, 0.5 mg/ml streptomycin sulfate, and 50 μM 2-mercaptoethanol (Sigma Chemical, St. Louis, MO, USA) in a 5 % CO2 humidified incubator. C57/BL6 female mice (6–8 weeks old, 17–21 g) were obtained from Yang Zhou University (Yangzhou, China).

Peptide synthesis

BP5 (Cys-Lys-Asp-Val-Tyr) and BP5 analog (Ala-Lys-Asp-Val-Tyr) were synthesized by Shanghai Taishi Bioscience Co, Ltd (People's Republic of China) and analyzed by HPLC and electro spray ionization tandem mass spectrometry (ESI-MS/MS) mass spectrometry to confirm that the purity was higher than 95 %. All peptides were dissolved in water. To exclude lipopolysaccharide (LPS) contamination, both peptides were tested using the E-Togate Limulus LPS detection kit (Sigma Chemical Co.).

CFU pre-B assay

Single-cell suspensions were obtained from the Bone marrow of C57/BL6 mice at the age of 4–6 weeks. Cells were suspended in Iscove's Modified Dulbecco's Medium containing 1 % Methylcellulose, 2 mM L-glutamine, 10 % fetal calf serum (FCS), 50 μM 2-mercaptoethanol, 0.1 g/L streptomycin, and 10^5 U/ml penicillin. Whole Bone marrow cells were treated with the IL-7(10 ng/ml) and BP5, mixed with Methylcellulose, and plated in 35-mm culture dishes. The plates were incubated at 37 °C, 5 % CO2. Colonies containing at least 40 cells were counted as described (Fine et al. 2009). Data were presented as the mean number of CFU/1.25 × 10^4 cells for triplicate samples ± SD.

Cell collection

WEHI-231 cells (1 × 10^7) were treated with or without BP5 (5 μg/ml) for 48 h, and then were manually washed in phosphate buffered saline at 37 °C. Then they were manually washed in phosphate buffered saline at 37 °C to remove any residual host proteins. The samples were designated as control and BP5, respectively.

Protein extraction

Lysis buffer (pH 8.5) containing 7 M urea, 2 M thiourea, 65 mM Tris, 2 % dithiothreitol (DTT), 4 % 3-[(3-cholamidopropyl) dimethylammonio] propanesulfonate (CHAPS), 0.2 % IPG buffer (GE Amersham Biosciences, now GE Healthcare, Chalfont St. Giles, Buckinghamshire, UK) and 0.1 % (v/v) protease inhibitor mixture (Merck, Darmstadt, Germany) was added into cell samples. Cell disruption was achieved by sonication at 80 W for 10 s ×5

with intervals of 15 s, followed by the addition of lysis buffer to a final volume of 1 ml. Samples were maintained on ice during these procedures. The mixture was then centrifuged at 12,000 rpm for 40 min at 4 °C to remove insoluble material. The protein content in the supernatant was quantified by the Bradford method using Bio-Rad protein assay reagent. Samples of aliquots were stored at 80 °C until use in proteomic analysis.

2D-E

An equal volume of rehydration buffer (8 M urea, 4 % CHAPS, 2 % DTT and 2 % IPG buffer pH 3–10) was added to total proteins (80 μg each) so that the final concentration of DTT and IPG buffer was 1 %. The protein samples were subjected to isoelectric focusing carried out on nonlinear IPG strips, 13 cm long, pH 3–10 (GE Healthcare), rehydrated at 30 V for 12 h at room temperature. Isoelectric focusing was conducted at 500 V for 1 h, followed by 1,000 V for 1 h, then 8,000 V 10 h to reach a total of 60–80 Kvh using the Ettan II IPG-phor apparatus (GE Healthcare).

After the IEF run was completed, strips were equilibrated under gentle shaking in two steps of 10 min each, first in equilibration buffer I (1 % DTT, 50 mM Tris–HCl, pH 6.8, 6 M Urea, 30 % Glycerol, 2 % SDS bromphenol blue) and then in equilibration buffer II (same as equilibration buffer I, except that DTT was increased to 2.5 %,). Equilibrated strips were loaded onto a 12.5 %, pH 8.8, 13 cm polyacrylamide gel with a 1 cm, 4 %, pH 6.8 stacker gel. The separated proteins were visualized by silver diamine staining. For reparative 2D-E, 400 mg of total proteins was separated as described above. Proteins were detected by a modified silver-staining method compatible with MS analysis.

Visualization

The silver-stained 2-D gels were scanned by a GS-710 imaging densitometer. The digitized images were analyzed with the Image Master software (GE Health care). A reference gel was selected from one of the gels and unmatched protein spots of the member gels were automatically added to the reference gel.

Tryptic digestion

Protein spots were cut from gels, destained for 20 min in 30 mM potassium ferricyanide/100 mM sodium thiosulfate (1:1 v/v) and washed in Milli-Q water until the gels were destained. The spots were kept in 0.2 M NH_4HCO_3 for 20 min and then lyophilized. Each spot was digested overnight in 2 μl 12.5 ng/μl trypsin in 0.1 M NH_4HCO_3. The tryptic peptides were extracted three times with 50 % acetonitrile, 0.1 % trifluoroacetic acid and dried completely by centrifugal lyophilization.

Matrix-assisted laser desorption ionization (MALDI)-Time-of-flight (TOF) MS analysis, database searches, and bioinformatics analysis

The tryptic peptide samples were sent to Shanghai GeneCore Bio-Technologies Co. Ltd. for MALDI-TOF–MS peptide mass fingerprint analysis. Peptide mass fingerprint dates were submitted to MASCOT Sequence Query server (http://www.matrixscience.com) for identification against nonredundant NCBI database (http://www.ncbi.nlm.nih.gov/BLAST). Identification required a MASCOT confidence interval of 95 %. The other search parameters were: cleavage enzyme, trypsin; fixed modification, carbamidomethyl (C); variable modifications, oxidation (M); max missed cleavage, 1. Peptide tolerance of 100 ppm; fragment mass tolerance of ±0.5 Da; and a peptide charge of 1+ were considered significant. The criteria used to accept protein identifications were based on the data of peptide mass fingerprint, including the extent of sequence coverage, number of peptides matched and probability score. Only high-scoring proteins were accepted. Gene ontology (GO) annotations for identified proteins based on BLAST results were performed using Blast2GO (www.blast2go.de) and AmiGO (http://amigo.geneontology.org/cgi-bin/amigo/go.cgi). The Blast2GO software was also used to complement multiple identified proteins within the Kyoto Encyclopedia of Genes and Genomes metabolic pathway maps (www.genome.jp/kegg/).

Fluorescence microscopy and flow cytometry

WEHI-231 cells were treated with or without FITC-BP5 for 2 h. After fixation in 80 % ice-cold acetone at −20 °C for 10 min, cells were stained with 4′,6-diamidino-2-phenylindole (DAPI) for 10 min. After being washed, cells were detected with Zeiss Axiovert 200 microscope (Zeiss, Oberkochen, Germany) equipped with Spot RT KE digital camera.

WEHI-231 cells were treated with FITC-BP5 or FITC for 2 h, then Samples were kept at 4 °C in the dark and analyzed by flow cytometry (Cytomics FC500 MPL flow cytometry system, Beckman Coulter, Fullerton, CA, USA). A total of 10, 000 cells were analyzed for each sample.

ROS measurement and GSH content

The intracellular reactive oxygen species (ROS) was assessed fluorometrically. Briefly, Bone marrow cells

(1×10^6 /ml) from C57/BL6 mice were cultured with IL-7 (10 ng/ml) for 4 days to enrich B cells. Next, these cells were collected and cultured with or without 1, 5, 25 μg/ml BP5 for 24 and 48 h, then washed with serum-free RPMI culture medium and incubated with 5 μmol/l dichlorofluorescein diacetate (DCFH-DA, Beyotime, Hangzhou, China) at 37 °C for 30 min. The fluorescence intensities of 1×10^4 cells from each sample were analyzed by flow cytometry (Cytomics FC500 MPL flow cytometry system, Beckman Coulter, Fullerton, CA, USA) for 30 min. The WEHI-231 cells (1×10^6 /ml) were cultured with or without 1, 5, 25 μg/ml BP5 or H_2O_2 (30 μM) for 24 and 48 h, then measured the intracellular ROS with the method given above. Total content (T-GSH), GSH and GSSG were measured spectrophotometrically according to the commercial assay kit procedure (Beyotime, Hangzhou, China).

Cell viability

WEHI-231 cells were added to 96-well flat-bottomed microtiter plates (100 μl/well of 2×10^5 cells/ml) in medium adding 10 % FCS, and were stimulated by BP5 with 1, 5 and 25 μg/ml for 48 h. At least six replicated wells per sample were prepared, and control cultures without sample were included. The cell viability was measured after 24, 48 and 72 h using the WST-1 Cell proliferation and cytotoxicity assay kit (Beyotime, Hangzhou, China) in accordance with the manufacturer's instructions. Briefly, 10 μl of this reagent was added to each well containing 100 μl of cell suspension incubated for an additional 1 h. The absorbance at 450 nm was monitored and the reference wavelength was set at 630 nm. The percent viability of cells was calculated by comparison to that of untreated control cells.

Western blot

Western blotting was performed as previously described (Qiu et al. 2008) using anti-G6PD monoclonal antibody (G6PD, Santa Cruz, USA) and β-actin (Beyotime, Hangzhou, China).

Real-time PCR

Total RNA was isolated using the TRIzol Reagent (Invitrogen). DNA-free total RNA (100 ng) was subjected to cDNA synthesis using PrimeScript® RT reagent Kit (TaKaRa Bio Inc, Shiga, Japan) according to the manufacturer's instructions. Real-time polymerase chain reaction (PCR) was performed in a Light Cycler instrument (Eppendorf, German) in a total volume of 20 μl using the SYBR® Premix Ex Taq™ (Perfect Real Time) kit (TaKaRa Bio Inc, Shiga, Japan) according to the manufacturer's instructions. The primer sets fors elected genes are shown in Table 1.

G6PD activity

G6PD activity was measured at 37 °C according to Beutler's method, which depends on the reduction of $NADP^+$ by G6PD, in the presence of glucose 6-phosphate. The activity measurement was made by monitoring the increase in absorption at 340 nm due to the reduction of $NADP^+$ at 37 °C. One enzymatic activity unit was defined as the reduction of 1 μmol of $NADP^+$ per minute at 37 °C and pH 8.0 (Beutler 1975).

γ-H2AX foci

WEHI-231 cells were plated on BD-Falcon culture slides chamber and treated as indicated in the text. Cells were fixed in 95 % EtOH/5 % acetic acid and stained with anti-phospho-H2AX (ser139) antibody (Abgent) according to the manufacturer's instructions. The image was acquired on a Zeiss Axiovert 200 microscope (Zeiss, Oberkochen, Germany) equipped with Spot RT KE digital camera.

RNA interference

To silence G6PD, WEHI-231 cells were transfected with 50 pmol of G6PD stealth siRNA or control siRNA (Invitrogen) complexed with lipofectamin (Invitrogen) according to the manufacturer's instruction. The procedure was repeated after 24 h from the first transfection to get the maximum silencing of the gene. The nucleotide sequences of G6PD siRNA were 5′-CUGGAAACUUACACCAUCU-3′ (sense) and 5′-AGAUGGUGUAAGUUUCCAG-3′ (antisense).

Statistical analysis

Results were expressed as means ± standard deviations (SD). The statistical significance of the observed differences was analyzed by 2-sided *t* test unless otherwise specified. *P* value <0.05 was considered to be significance level.

Result

BP5 promoted CFU pre-B formation and affected the redox homeostasis of B cells

Considering that BP5 enhanced anti-hemagglutinin antibody production, induced both of Th1 and Th2-type cytokines,

Table 1 Primer sequences of target genes

Differentially expressed protein	Forward primers (5′–3′)	Reverse primers (5′–3′)
Pgk1	CAACCAGATAACGAATAACCAAAGG	CCAGGTGGCTCATAAGCACAA
G6PD	GAAAGCAGAGTGAGCCCTTC	CATAGGAATTACGGGCAAAGA
Atp5a1	CAAGCCTTGTTGGGCACTAT	AGCTTCAAATCCAGCCAAGA
Atp5b	GCAAGGCAGGGACAGCAGA	CCCAAGGTCTCAGGACCAACA
Psma3	TCTTGCAGACAGAGTGGCCA	CGCACTGTAAGACCCCAACA
Psma4	TCTGCACCCTCACCGTCTTC	TCTCGAAGATATGACTCCAGGAC CACAATATTTTCT
Sfrs1	CACTGGTGTCGTGGAGTTTG	CTTCTGCTACGGCTTCTGCT
GAPDH	GTCAACGGATTTGGTCGTATT	GATCTCGCTCCTGGAAGATGG

Transcript levels were normalized relative to those of GAPDH

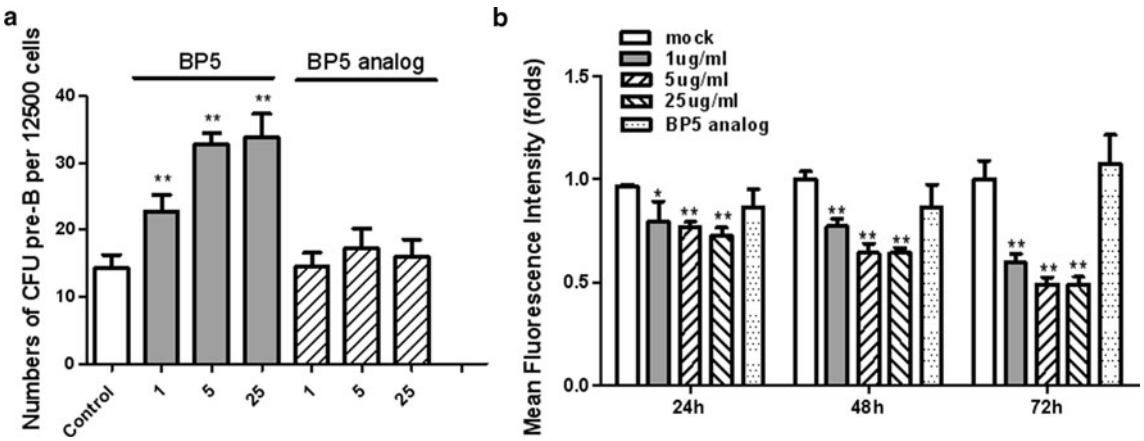

Fig. 1 Role of BP5 in CFU pre-B formation and intracellular ROS production in Bone marrow B cells **a** role of BP5 in CFU pre-B formation. Bone marrow cells were plated in 35-mm dish at 1.25×10^4 cells in methylcellulose medium. Various concentrations of BP5 and BP5 analog (from 1 to 25 μg/ml) were added in the culture. In the control group, the cells were treated with BSA (1 μg/ml). The cells were cultivated for 7 days and the produced colonies (CFU pre-B) were scored. $^*P < 0.05$, $^{**}P < 0.01$. **b** Role of BP5 and BP5 analog in intracellular ROS production in Bone marrow B cells. The ROS levels in the culture of Bone marrow B cells were measured using the redox sensitive fluorescent dye carboxy-2′,7′-dichlorofluorescein diacetate (DCF-DA, a reliable fluorogenic marker for ROS, Biyuntian), and the fluorescence intensities of 1×10^4 cells were analyzed by flow cytometry. $^*P < 0.05$, $^{**}P < 0.01$. *Error bars* indicate mean ± SD, $n = 3$ for each

increased proliferations of splenic lymphocytes, we investigated the possibility that BP5 regulates B cell development. We used the CFU pre-B formation assays to investigate the roles of BP5 in B cell development. Bone marrow cells (1×10^6 cell/ml) from C57/BL6 mice were plated in methylcellulose supplemented in the presence of IL-7(10 ng/ml) and with or without BP5 at concentrations from 1 to 25 μg/ml, for 7 days. There were 14 colonies per 12,500 cells in the presence of IL-7. The counts of colonies with IL-7 and BP5 treatment were more than those in IL-7 treated groups. However, when Cys of BP5 was replaced by Ala in BP5 analog, the counts of colonies were no more than those in IL-7 treated groups (Fig. 1a). These results exerted that BP5 could promote CFU pre-B, and Cys played an important role.

As Cys may affect the ROS (Sato et al. 1999; Banjac et al. 2008), and the reduced environment is essential to B cell development (Ruprecht and Lanzavecchia 2006), so we were interested in the role of BP5 in intracellular generation of ROS in Bone marrow B cells. To investigate whether BP5 could regulate intracellular ROS production, the ROS levels in the culture of Bone marrow B cells were measured using the redox sensitive fluorescent dye carboxy-2′,7′-dichlorofluorescein diacetate (DCF-DA, a reliable fluorogenic marker for ROS). As shown in Fig. 1b, the ROS production was significantly decreased by BP5 (1–25 μg/ml) relative to the control group. Interestingly, BP5 analog had no effect of the ROS production of Bone marrow B cells. These data indicated that BP5 regulated the redox homeostasis of B cells, which were associated with its special amino acid sequence.

The effect of BP5 on WEHI-231 cell line model

To investigate the mechanisms through which BP5 acted on the intracellular ROS production, we chose WEHI-231 cells, an immature B cell line, as model system.

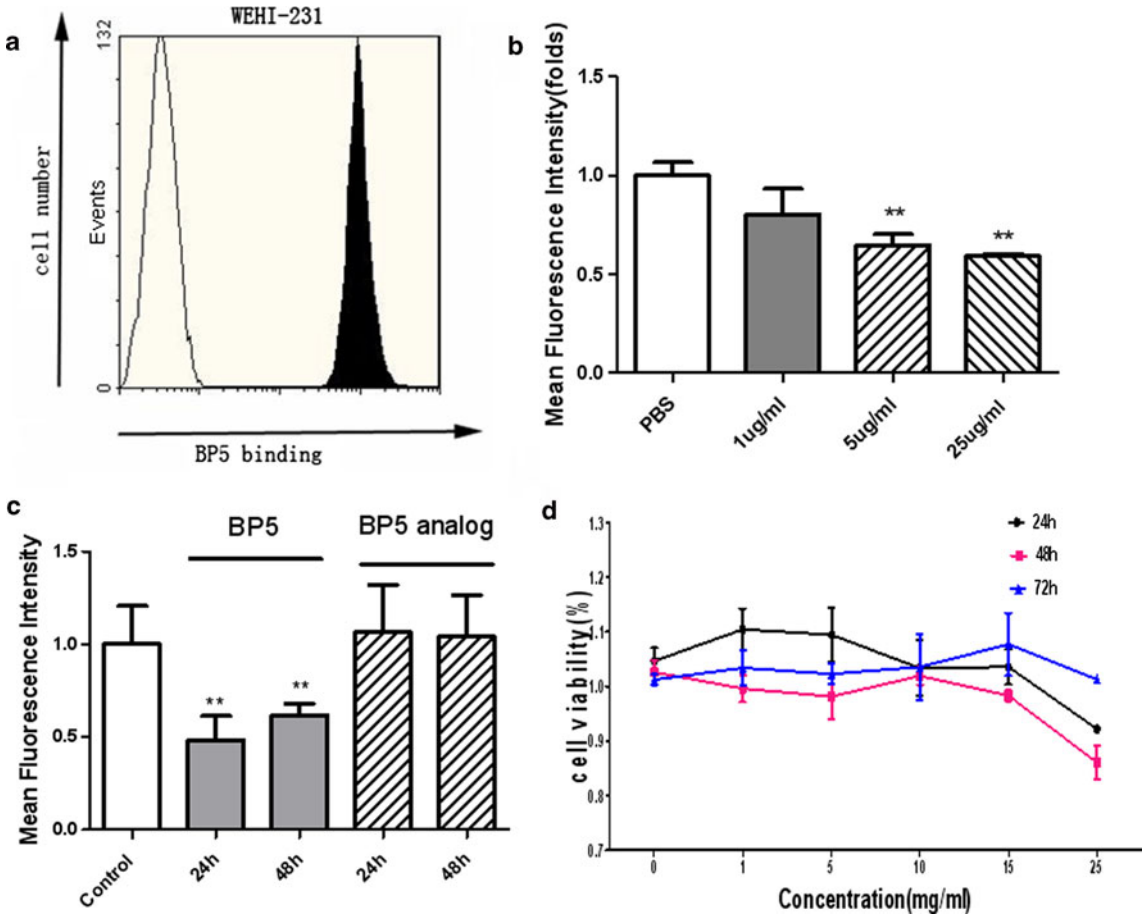

Fig. 2 Role of BP5 in WEHI-231 cells. **a** WEHI-231 cells were treated with or without FITC-BP5 for 2 h, and then detected by FACS. FITC-BP5 (*shaded*) and FITC only (*bold line*) traces are shown. Results shown are from one of three experiments. **b** Mean fluorescence intensity of cells treated with or without 1, 5 and 25 μg/ml BP5 for 24 h. **c** Mean fluorescence intensity of cells treated with BP5 (5 μg/ml) or 5 μg/ml BP5 analog for 24 and 48 h. **d** WEHI-231 cells viability was measured by WST-1 assay at absorbance 450 nm. The data of samples without BP5 treatment (Control) were used as basic control, and other treatment data (BP5 1, 5 and 25 μg/ml) were compared to that. $*P < 0.05$. *Error bars* indicate mean ± SD, $n = 3$ for each

First, FITC-BP5 was used to investigate binding to WEHI-231 cells. we found that BP5 could bind WEHI-231 cells by Flow cytometry analysis (Fig. 2a). Also, these results were observed in other cells (data not shown). Then we investigated the intracellular ROS production of WEHi-231 cells after BP5 treatment. It was observed that the intracellular ROS production decreased with BP5 treatment in a dose and time-dependent manner (5 μg/ml BP5, $P < 0.05$; 25 μg/ml BP5, $P < 0.01$), which was consistent with results of Bone marrow B cells. Many molecules which have antioxidant activity are toxic, may affect cell viability (Munday 1989), As an antioxidant, we wanted to determine the effects of BP5 on WEHI-231 cell viability. The results showed that BP5 do not affect cell viability at concentrations of 1, 5, 10, 15 μg/ml, and slightly inhibits the cell viability at concentrations of 25 μg/ml (Fig. 2d).

Various processes are involved in BP5-regulated B lymphocyte cell

To further study the mechanism of BP5 on the regulation of the B cells, the two-dimensional gel electrophoresis profiles was applied. Soluble proteins extracted from the WEHI-231 cells treated with or without BP5 were compared with the 2D-E technique. The analysis of 2D-E revealed 40 spots with a statistically significant (t test, $p < 0.01$) change in intensity of >1.3 (Fig. 3).

The proteins selected as differentially expressed were separated on a preparative gel and visualized by staining with Coomassie blue. Gel pieces containing the proteins of interest were excised and subjected to digestion with trypsin. Thus, 40 protein spots were selected for analysis with MALDI MS/MS, based on the amount of protein, matching across gels, and the presence of the protein spot

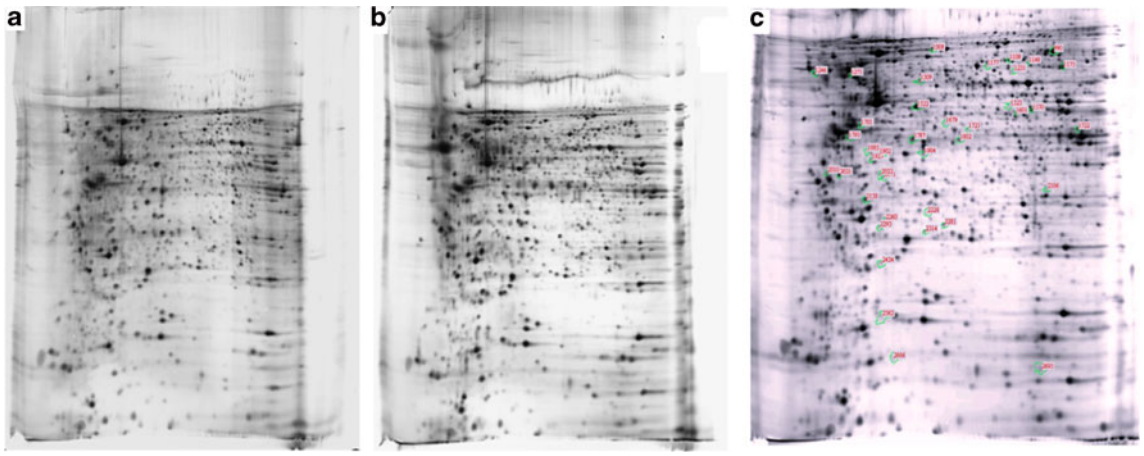

Fig. 3 Two-dimensional gel electrophoresis profiles of BP5-treated WEHI-231 cells. Proteins extracted from BP5-treated WEHI-231 cells (**a**) and untreated WEHI-231 cells (**b**) were separated on preparative gel visualized by Coomassie brilliant blue staining. **c** Differentially expressed proteins of BP5 group and control (*green marked*). Three positive controls of known concentration were included in every run to confirm consistent amplification. Quantization of relative differences in expression was calculated using the Rotor-Gene version 6.0.38 software (Corbett Research, Australia) (color figure online)

on the preparative gels. Among them, 22 proteins were successfully identified and are listed in Table 2.

To better understand the biological functions of the differentially expressed proteins, GO Annotation was performed. Each identified known protein was classified according to its Go functional annotation. These differentially expressed proteins were principally involved in oxidoreduction coenzyme metabolic process, precursor metabolites and energy, proteolysis, RNA splicing and translation and cellular process (Fig. 4a).

Seven genes corresponding to the up-regulated proteins and down-regulated proteins Pgk1, G6PD, Atp5a1, Atp5b, Psma3, Psma4 and Sfrs1 were chosen for quantitative real-time PCR (qPCR) analysis to quantify their transcript levels (Fig. 4). The qPCR results were consistent with that of the 2D-E results, which suggested that these proteins identified as differentially expressed were regulated at transcriptional level (Fig. 4b).

BP5 enhanced G6PD expression and activity

G6PD, the first and rate-limiting enzyme in the pentose phosphate pathway (PPP), is an important source of cellular NADPH, which is essential in the regulation of anti-oxidant systems. We found that G6PD was up-regulated in cells after BP5 treatment through 2D-E gels. Western blot analysis was performed to detect the expression of G6PD. The data showed that trends of difference of protein expression in immunoblots between BP5 treated and control WEHI-231 cells were consistent with the data in 2D-E gels (Fig. 5a). In Bone marrow B cells, BP5 also enhanced the expression of G6PD at transcriptional level (Fig. 5c).

To further understand how BP5 acts on G6PD, we examined the G6PD activity in the presence of BP5 treatment. Interestingly, we found that BP5 could enhance the G6PD activity, which might partly explain the anti-oxidant activity of BP5 (Fig. 5b).

In addition, we found that the inactivation of G6PD increased ROS production. The suppressive effect on ROS production by BP5 was down-regulated after G6PD knock-down, the suppressive rate of BP5 on ROS production was 51.9 % at 24 h and 38.3 % at 48 h (Fig. 2c), while the suppressive rate of BP5 was 12.2 % at 24 h and 13.9 % at 48 h after G6PD knock-down (Fig. 6b). And the up-regulation of GSH/GSSG by BP5 in WEHI-231 cells was lost after G6PD knock-down (Fig. 6c–e). These results suggested that G6PD was an important part for BP5 in regulating the anti-oxidant environment, which partly explained the mechanism of BP5.

As G6PD activity is required for DNA repair, to verify BP5 is responsible for limiting the effects of ROS induced after DNA damage, we measured ROS production following H_2O_2 treatment. We found that BP5 had the suppressive effect on ROS production after H_2O_2 treatment ($P < 0.01$) (Fig. 7b). In addition, we used the γ-H2A foci formation to evaluate the effect of BP5 in DNA repair. The results showed that more γ-H2A foci were observed at 24 h after H_2O_2 treatment (30 μM); when treated with BP5 (5 μg/ml), the γ-H2A foci decreased, correlating well with the ROS results. These results suggested that BP5 could reduce DNA damage in WEHI-231 cells (Fig. 7).

Table 2 Identification of proteins differentially expressed between BP5-treated WEHI-231 cells and control: MALDI-TOF MS analyses

Spot ID	Database ID no.	Identified protein name	Protein name abbreviation	Protein PI	Protein MW	Protein score	Protein score CI %	Total ion score	Total Ion CI %	Count	Functional clustering
Up-regulated											
1177	IPI00320217	T-complex protein 1 subunit beta	cct2	5.97	57,783.2	551	100	426	100	17	Protein complex assembly protein folding
1523	IPI00555069	Phosphoglycerate kinase 1	Pgk1	8.02	44,921.1	170	100	82	100	14	Glycolysis
1108	IPI00228385	Glucose-6-phosphate 1-dehydrogenase X	G6pdx	6.06	59,680.9	440	100	314	100	19	Monosaccharide metabolic process
1701	IPI00759870	Heterogeneous nuclear ribonucleoproteins C1/C2	Hnrnpc	4.95	32,260.8	657	100	515	100	17	Nuclear mRNA splicing, via spliceosome
1802	IPI00227808	Isoform 1 of Protein CDV3	Cdv3	5.84	29,711.3	393	100	337	100	8	Unknown
1231	IPI00133916	Heterogeneous nuclear ribonucleoprotein H	Hnrnph1	5.89	49,453.5	251	100	151	100	14	Nuclear mRNA splicing, via spliceosome
1175	IPI00130280	ATP synthase subunit alpha, mitochondrial	Atp5a1	9.22	59,829.6	1,120	100	917	100	24	Cation transport nucleobase, nucleoside, nucleotide and nucleic acid metabolic process
Down-regulated											
2434	IPI00187407	COP9 signalosome complex subunit 8	Cops8	5.09	23,298	222	100	205	100	3	Proteolysis
2041	IPI00114407	Isoform 1 of THO complex subunit 4	Thoc4	11.15	26,923.6	225	100	189	100	7	Nucleobase, nucleoside, nucleotide and nucleic acid transport transcription from RNA polymerase II promoter
2293	IPI00988063	Triosephosphate isomerase	Tpi1	6.9	27,037.9	424	100	333	100	11	Glycolysis
2314	IPI00387502	26S proteasome non-ATPase regulatory subunit 10	Psmd10	5.68	25,352.8	394	100	305	100	10	Proteolysis
2562	IPI00649157	Stathmin	Stmn1	9.07	16,973.9	84	99.974	59	99.97	5	Intracellular signaling cascade, ectoderm development, nervous system development
1902	IPI00420807	Isoform 1 of Serine/arginine-rich splicing factor 1	Sfrs1	10.37	27,841.9	279	100	172	100	14	Nuclear mRNA splicing, via spliceosome
2260	IPI00110657	Isoform 2 of FGFR1 oncogene partner 2 homolog	2	5.44	25,048.8	363	100	188	100	18	Immune system process
2158	IPI00331644	Proteasome subunit alpha type-3	3	5.29	28,615.2	564	100	446	100	14	proteolysis

Table 2 continued

Spot ID	Database ID no.	Identified protein name	Protein name abbreviation	Protein PI	Protein MW	Protein score	Protein score CI %	Total ion score	Total Ion CI %	Count	Functional clustering
1570	IPI00153750	Nuclear inhibitor of protein phosphatase 1r	8	6.88	38,674.9	373	100	316	100	9	Signal transduction, RNA catabolic process, nuclear mRNA splicing, via spliceosome,signal transduction
2022	IPI00124103	Copper chaperone for superoxide dismutase	Ccs	5.7	29,463.6	110	100	88	100	5	Cation transport
2106	IPI00277001	Proteasome subunit alpha type-4	Psma4	7.59	29,737.3	109	100	73	99.999	6	Proteolysis
1275	IPI00468481	ATP synthase subunit beta, mitochondrial	Atp5b	5.19	56,265.5	498	100	381	100	16	Respiratory electron transport chain, purine base metabolic process
1927	IPI00474158	Isoform 3 of Serine/ arginine-rich splicing factor 7	Sfrs7	9.54	18,107	273	100	194	100	10	Nuclear mRNA splicing, via spliceosome
1601	IPI00626752	Mitotic checkpoint protein BUB3	Bub3	6.36	37,330.3	1,070	100	880	100	19	Mitosis, chromosome segregation
1148	IPI00466069	Elongation factor 2	Eef2	6.41	96,222.2	306	100	222	100	18	Translation

All the identified proteins matched with those in mus database

The spot ID was determined at the beginning of analysis of gels

The functions are classified by gene ontology (GO) annotations using Blast2GO and AmiGO

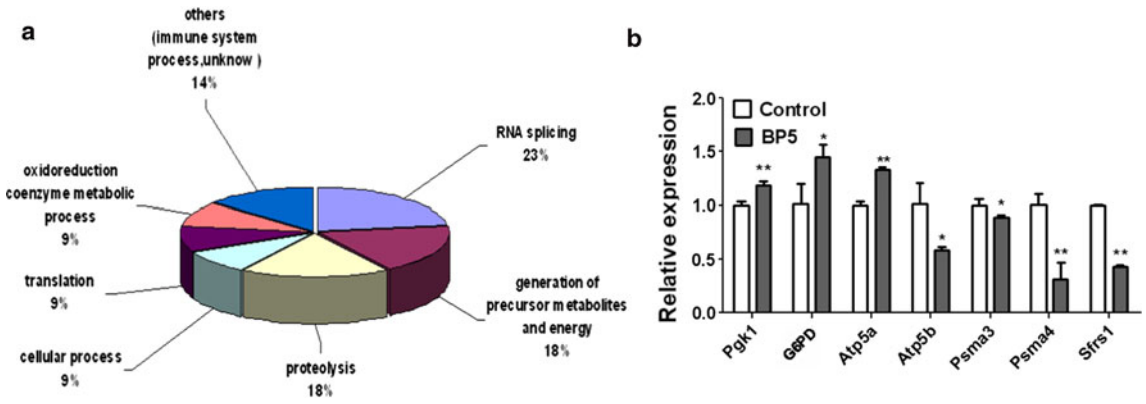

Fig. 4 Distribution of the identified proteins according to GO analysis and Quantitative Real-time PCR Analysis of Differentially Expressed Proteins. **a** Distribution of the identified proteins according to GO analysis. Assignments were made on the basis of information provided by GO lists downloaded from AMIGO (http://www.godatabase.org/cgi-bin/amigo/go.cgi). **b** Quantitative Real-time PCR Analysis of Differentially Expressed Proteins. The total cellular RNA with or without BP5 treated was subjected to real-time RT-PCR analysis. Transcript levels corresponding to seven out of 22 differentially expressed proteins were presented relating to that of GAPDH. *Error bars* indicate mean ± SD, $n = 3$ for each

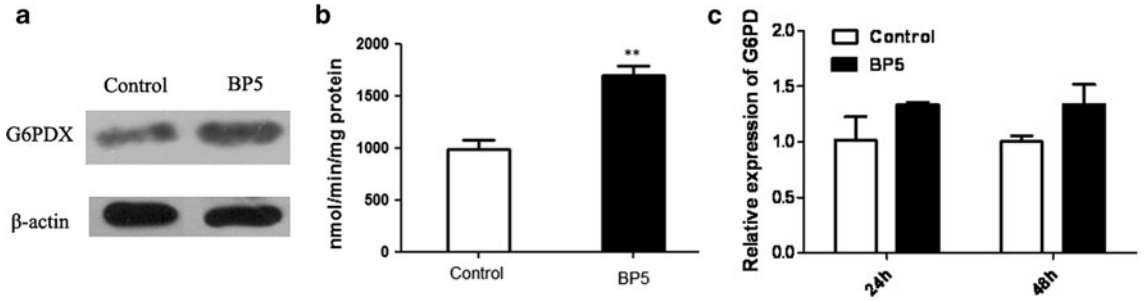

Fig. 5 BP5 enhanced G6PD expression and G6PD activity. **a** BP5 enhanced G6PD expression. 20 μg of total protein from WEHI-231 cells with or without BP5 treated was separated by SDS-PAGE and analyzed by western blot anti-G6PD (*upper panel*) and β-actin (*bottom panel*). The enhanced G6PD expression after BP5 treated was consistent with results from 2D-E-MS/MS. **b** Glucose 6-phosphate dehydrogenase (G6PD) activity in control and BP5-treated WEHI-231 cells. **c** BP5 enhanced G6PD expression in Bone marrow B cells at transcript levels

Discussion

B-lymphocytes are exposed to a reduction/oxidation environment during the activation or inflammatory process. Proliferation, survival and differentiation of B lymphocytes require antigenic challenge and co-stimulatory signals (Ruprecht and Lanzavecchia 2006). On the other hand, an excess of ROS may cause an oxidative stress that leads to cell damage, with lipid peroxidation and disruption of structural proteins, enzymes, and nucleic acids (Cooke et al. 2003). The antioxidant systems are functional to protect cells against harmful ROS. Bursopentin (BP5, Cys-Lys-Asp-Val-Tyr) was isolated from chicken bursa of Fabricius, and proved to be a multi-functional modulator in immune response. As a new thiol-containing pentpeptide, which contains a cysteine in the N-terminal, BP5 regulated the ROS of spleen B cells (Li et al. 2011), both showing pro-oxidant effects and anti-oxidant effects. In murine peritoneal macrophages, BP5 could protect LPS-activated cells from oxidative stress (Li et al. 2012). In this study, BP5 was investigated in Bone marrow B cells and WEHI-231 B cell line to evaluate the effects of BP5 on B cell development and the redox homeostasis.

The CFU-pre B cell assay is useful in B cell development evaluation (Hardy et al. 1991). The results of our studies suggested that BP5 promoted IL-7-induced CFU pre-B formation, and Cys played an important role. BP5 also up-regulated the redox homeostasis of Bone marrow B cells at different concentrations. These results suggested that the antioxidant systems were important for B cell development, and the regulation of the redox homeostasis by Cys played an important role in the immune functions of BP5.

To determine the mechanisms involved in BP5 regulation of the redox homeostasis, we used the WEHI-231 B cells, an immature B cell line model. The results showed that BP5 down-regulated the ROS in WEHI-231 cells but did not affect WEHI-231 viability. We also found that BP5 had the ability of binding cells. It is conceivable that BP5

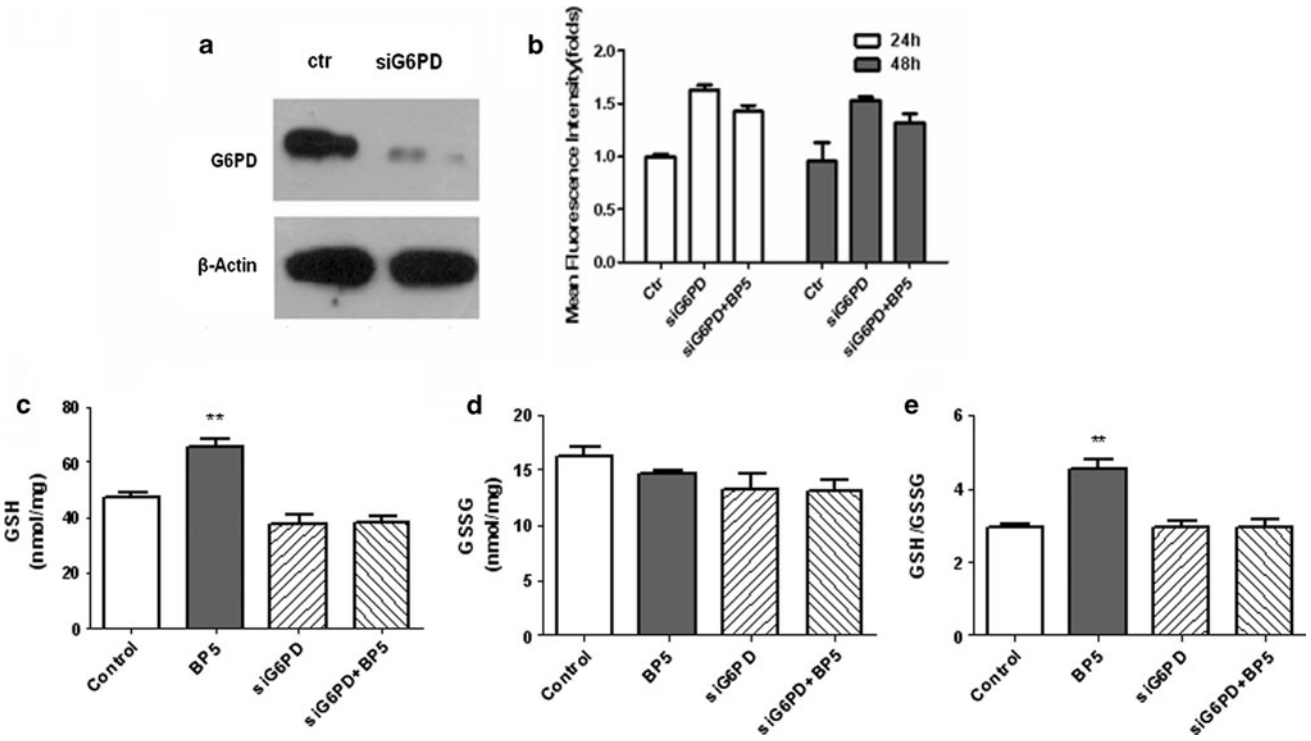

Fig. 6 Role of BP5 upon G6PD silencing. **a** Cells were transfected with a scrambled siRNA (ctr) and G6PD targeting siRNA. 20 μg of total protein was separated by SDS-PAGE and analyzed by western blot anti-G6PD (*upper panel*) and β-actin (*bottom panel*). **b** Mean fluorescence intensity of cells treated with or without G6PD targeting siRNA (siG6PD) and BP5 (5 μg/ml). **c** WEHI-231 cells (1×10^6 / ml) were treated with or without G6PD targeting siRNA (siG6PD) for 24 h. The levels of GSH, GSSG (D), and the ratio of GSH/GSSH (E) in the cells were measured using commercial Kits. Results shown were from one of three experiments. *Error bars* indicated mean ± SD, $n = 3$ for each

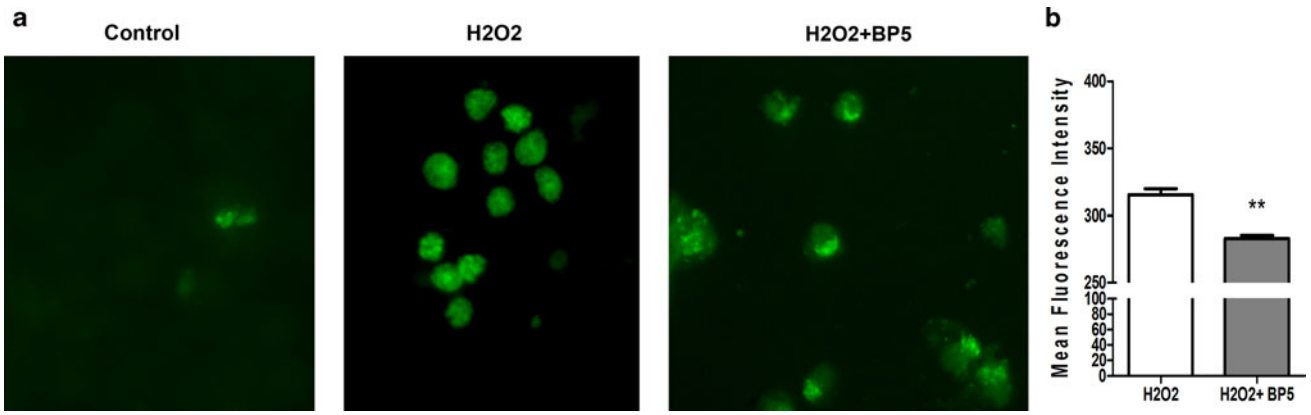

Fig. 7 Role of BP5 upon H_2O_2 treated. WEHI-231 cells were treated with or without H_2O_2 (30 μM) for 24 h, and γ-H2AX foci were visualized by immunofluorescence (**a**). **b** Mean fluorescence intensity of cells treated with or without H_2O_2 (30 μM) and BP5 (5 μg/ml). Results shown were from one of three experiments. *Error bars* indicated mean ± SD, $n = 3$ for each

could contribute to maintaining and reducing microenvironment.

2-D has been proved to be a powerful proteomics technique for the detection and identification of proteins differently expressed. In this paper, we performed a comparative proteomic analysis of proteins of WEHI-231 cells after BP5 treatment. The results showed that there were 22 proteins differently expressed between BP5-treated WEHI-231 cells and control cells. Go analysis revealed that most of the differentially expressed proteins were involved in a wide variety of cellular processes, including oxidoreduction coenzyme metabolic process, precursor metabolites and energy, proteolysis, RNA splicing and translation and cellular process.

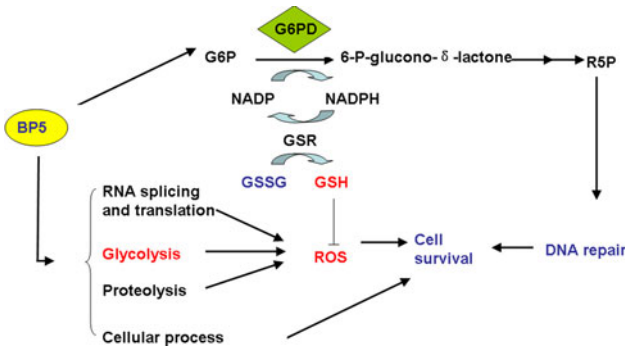

Fig. 8 Schematic representation of BP5 regulation effect. BP5 increases the activity of G6PD and the stimulation of the PPP. BP5 also regulates glycolysis, proteolysis, RNA splicing and translation and cellular process. As a consequence of these events, ROS levels are reduced and the dNTP pool is increased, promoting DNA repair and cell survival

G6PD, the first and rate-limiting enzyme in the PPP, is an important source of cellular NADPH. In this manner, G6PD contributes to the maintenance of cellular redox homeostasis by reducing equivalents for efficient GSH reductase activity and GSH recycling (Leopold et al. 1989). In this paper, the proteomics assay showed that BP5 up-regulates the expression of G6PD, and increases enzyme activity to a similar degree, suggesting that the increases in activity may be due to the increased protein levels. Inducing G6PD may cause the stimulation of the PPP, which in turn promotes NADPH production, then the GSSG quickly reduces back to GSH with reduced NADPH, and the highly reactive ROS are converted to more stable molecules. Therefore, the increases in GSH content and GSH/GSSG ratio caused by BP5 may promote NADPH production, and decrease intracellular oxidative stress. These effects of BP5 were down-regulated after G6PD knock-down in WEHI-231 cells, which suggests that G6PD was an important part for BP5 in regulating the anti-oxidant environment. G6PD was also required for efficient DNA repair by increasing the dNTPs pool needed to repair DNA (Leopold et al. 1989); we found that BP5 could also reduce DNA damage in WEHI-231 cells. These results indicated that BP5 may have increased dNTPs pool by promoting G6PD activity, the mechanism needs to be further studied.

There were various proteins regulated after BP5 treatment that are involved in generation of precursor metabolites and energy. TPI1 and PGK1 are enzymes associated with the glycolysis. TPI catalyzes the interconversion of glyceraldehyde 3-phosphate (G3P) and dihydroxyacetone phosphate (DHAP) which are 3-carbon units that are cleaved from 6-carbon units and which are useful for generating ATP. Some studies reported that antioxidant reduced Protein Kinase C directly or indirectly (Gopalakrishna 2002), which probably reflects decreased DHAP levels. The decreased DHAP is involved in glycerol synthesis, and impaired glucose metabolism. Other studies have reported a late activation of the PPP and a contemporary inhibition of the glycolysis sustained by P53 through TIGAR and NF-κB (Kawauchi et al. 2008). In our study, BP5 may inhibit the glycolysis, and cause the decrease in the TPI level. This inhibition of glycolysis might be important to reduce ROS, which is produced by glycolytic metabolism. Moreover, the decreased ROS induced the PGK expression increases via the down-regulated PKC pathway resulting in the decreases in the TPI expression during BP5 treatment.

Some antioxidants have effects on ATP production (Dave et al. 2008). The coupling step of the ATP biosynthesis in mitochondria is generally believed to involve an energy-requiring release of ATP bound to ATP5B. Molecular description by mutational analysis on ATP binding site in ATP5B has revealed its critical role in energy metabolism process (Thomas et al. 1992). ATP5A1 is part of the F1 enzymatic complex known to bind ADP, phosphate, and ATP and acts as a central part in the mitochondrial energy-producing mechanism (Yotov and StArnaud 1993). ATP5b and ATP5a1 are also the targets of other intracellular transducers, effectors, and modulators. In the present study, ATP5A1 is up-regulated and ATP5B is down-regulated. The changes in regulation between the two subtypes do not correlate, suggesting that there might be other factors to affect the specific subtype expression levels.

In eukaryotic cells, the turnover of intracellular proteins is mediated primarily by the ubiquitin–proteasome system (Coux et al. 1996). The 26S proteasome is a complex of ubiquitin–proteasome proteolytic pathway responsible for degradation of proteins that are naturally unfolded, mutated, or oxygen-damaged (Orlowski and Wilk 1996; Foss et al. 1998). There are few reports concerning the regulation of expression of proteasome subunits in mammalian cells. Expression of PSMB8, PSMB9, and PSMB10 is enhanced by gamma interferon and LPS exposure (Yoo and Desiderio 2003). Takabe et al. (2001) reported that the antiatherogenic antioxidant probucol repressed expression of PSMA2, PSMA3, and PSMA4. Very recently, Meiners et al. (2003) demonstrated that the proteasome inhibitor MG132 increases the expression of a broad range of subunits of the proteasome in mammalian cells. In this study, the 26S proteasome subunit beta type 3 and, the 26S proteasome subunit beta type 4 and the 26S proteasome subunit beta type 10 were found to be down-regulated. Though down-regulation of subunit beta type 3, 4 and 10 seems unrelated to the protease activity provided by subunit beta types 1, 2, and 5 Coux et al. (1996), we deduce that the expression of these active subunits are also likely down-

regulated although they were not identified in the present work.

COP9 signalosome complex subunit 8 is the smallest of the eight subunits of COP9 signalosome, a highly conserved protein complex that functions as an important regulator in multiple signaling pathways (Chamovitz and Deng 1995). The structure and function of COP9 signalosome are related to that of the 19S regulatory particle of 26S proteasome. COP9 signalosome has been shown to interact with SCF-type E3 ubiquitin ligases and act as a positive regulator of E3 ubiquitin ligases. Alternatively spliced transcript variants encoding distinct isoforms have been observed (Groisman et al. 2003). In this study, the Cpos8 was found to be down-regulated, which was consistent with the down-regulation of 26S proteasome subunit.

In this paper, it was identified that several genes were involved in RNA splicing and translation that are preferentially expressed. SFRS1, SFRS7, Ppplr8 and EEF2 were down-regulated, hnRNPs C1/C2 and Hnrnph1 were up-regulated. Elongation factors are a set of proteins that facilitate the events of translational elongation, the steps in protein synthesis from the formation of the first peptide bond to the formation of the last one. Elongation is the most rapid step in translation. Human hnRNP C1/C2 are members of the heterogeneous nuclear ribonucleoprotein family, which consists of 20 major hnRNP proteins with molecular sizes of 36–120 kDa (Piñol-Roma 1997). As pre-mRNA splicing emerges as a central mechanism to integrate cellular and metabolic stresses (Biamonti and Caceres 2009), the changes of these molecules in BP5-treated WEHI-231 cells could adversely affect the redox homeostasis regulation of Bone marrow B cells, and also the ribonucleotide metabolism, transcription and translation processes of B cells.

Finally, there various proteins were involved in cellular process in WEHI-231 cells after BP5 treatment. Bub3 is a protein involved with the regulation of the Spindle Assembly Checkpoint (SAC); as one of the checkpoint proteins, Bub3 delays the irreversible onset of anaphase through direction of kinetochore localization during prometaphase (Taylor et al. 1998) to achieve biorientation. Stathmin is the founding member of a family of proteins that plays critically important roles in the regulation of the microtubule cytoskeleton, which involved with intracellular signaling cascade regulating cell proliferation, differentiation and function (Doye et al. 1989). T-complex protein1 sub-unit beta (CCT2) is responsible for actin and tubulin folding during cell proliferation, and vimentin (VIM) contributes to the structural stability. Here, we identified that BUB3 and Stathmin proteins were down-regulated, whereas CCt2 was up-regulated significantly after BP5 treatment. Though BP5 did not affect WEHI-231 proliferation, these dates suggested the potential effect of BP5 on kinetochores, microtubule cytoskeleton, regulating cell cycle.

In summary, our current work suggests that BP5 markedly promoted B cell development by increasing CFU-pre B, and affected the redox homeostasis regulation of B cells. BP5 affected the redox homeostasis regulation of WEHI-231 cells through regulating expression of G6PD, which in turn regulated the GSH redox cycle and various cellular processes, including oxidoreduction coenzyme metabolic process, precursor metabolites and energy, proteolysis, RNA splicing and translation and cellular process (Fig. 8). These data suggest that BP5 affected the redox homeostasis regulation by promoting the expression of G6PD, which in turn regulated the GSH redox cycle and other processes. The identification of these molecules provides a better understanding of the mechanism of action of BP5 in the regulation of B cells and suggests new therapies for the treatment of immune diseases. This study indicates that BP5 may have applications as a new reagent regulating cellular redox environment.

Acknowledgments This work was supported by the National Special Research Programs for Non-profit Trades, Ministry of Agriculture (No. 201203082), and National Natural Science Foundation(No. 31302067), and Jiangsu Natural Science Foundation(No. BK20130682), and a project funded by the Priority Academic Program Development of Jiangsu Higher Education Institutions (PAPD), and Youth Science and Technology Innovation Fund of Nanjing Agricultural University (No.KJ2013023). We also thank Shanghai Applied Protein Technology Co. Ltd. for the technology support.

Conflict of interest The authors declared no conflicts of interest.

References

Angelini G, Gardella S, Ardy M, Ciriolo MR, Filomeni G, DiTrapani G, Clarke F, Sitia R, Rubartelli A (2002) Antigen-presenting dendritic cells provide the reducing extracellular microenvironment required for T lymphocyte activation. Proc Natl Acad Sci 99:1491–1496

Audhya T, Kroon D, Heavner G, Viamontes G, Goldstein G (1986) Tripeptide Structure of bursin a selective B-cell-differentiating hormone of the bursa of Fabricius. Science 231:997–999

Baba T, Kita M (1977) Effect of extracts of the bursa of Fabricius on IgG antibody production in hormonally bursectomized chickens. Immunology 32:271–274

Banjac A, Perisic T, Sato H, Seiler A, Bannai S, Weiss N, Kölle P, Tschoep K, Issels RD, Daniel PT, Conrad M, Bornkamm GW (2008) The cystine-cysteine cycle: a redox cycle regulating susceptibility versus resistance to cell death. Oncogene 27:1618–1628

Beutler E (1975) Red cell metabolism: a manual of biochemical methods, 2nd edn. Grune amd Stratton Inc., New York

Biamonti G, Caceres JF (2009) Cellular stress and RNA splicing. Trends in biochemical sciences. Cell 34(3):146–153

Brand A, Gilmour DG, Goldstein G (1976) Lymphocyte-differentiating hormone of bursa of Fabricius. Science 193:319–321

Castellani P, Angelini G, Delfino L, Matucci A, Ru-bartelli A (2008) The thiol redox state of lymphoid organs is modified by immunization: role of different immune cell populations. Eur J Immunol 38:2419–2425

Chamovitz DA, Deng XW (1995) The novel components of the Arabidopsis light signaling pathway may define a group of general developmental regulators shared by both animal and plant kingdoms. Cell 82:353–354

Cooke MS, Evans MD, Dizdaroglu M, Lunec J (2003) Oxidative DNA damage: mechanisms mutation and disease. FASEB J 17:1195–1214

Cooper MD, Peterson RD, South MA, Good RA (1966) The functions of the thymic system and the bursa system in the chicken. J Exp Med 123:75–102

Coux O, Tanaka K, Goldberg AL (1996) Structure and functions of the 20S and 26S proteasomes. Annu Rev Biochem 65:801–847

Dave M, Attur M, Palmer G, Al-Mussawir HE, Kennish L, Patel J, Abramson SB (2008) The antioxidant resveratrol protects against chondrocyte apoptosis via effects on mitochondrial polarization and ATP production. Arthritis Rheum 58(9):2786–2797

Davison F, Kaspers B, Schat KA (eds) (2008) Avian immunology. Elsevier Inc/Academic Press, New York

Doye V, Soubrier F, Bauw G, Boutterin MC, Beretta L, Koppel J, Vandekerckhove J, Sobel A (1989) A single cDNA encodes two isoforms of stathmin a developmentally regulated neuron-enriched phosphoprotein. J Biol Chem 264:12134–12137

Dröge W, Breitkreutz R (2000) Glutathione and immune function. Proc Nutr Soc 59:595–600

Fine JS, Macosko HD, Grace MJ, Narula SK (2009) Influence of IL-10 on murine CFU-pre-B formation. Exp Hematol 22(12): 1188–1196

Foss GS, Larsen F, Solheim J, Prydz H (1998) Constitutive and interferon-gamma-induced expression of the human proteasome subunit multicatalytic endopeptidase complex-like 1. Biochim Biophys Acta 1402:17–28

Glick B, Chang TS, Jaap RG (1956) The bursa of Fabricius and antibody production. Poult Sci 35:224–226

Gopalakrishna R (2002) Antioxidant regulation of protein kinase C in cancer prevention. J Nutr 132(12):3819–3823

Groisman R, Polanowska J, Kuraoka I, Sawada J, Saijo M, Drapkin R, Kisselev AF, Tanaka K, Nakatani Y (2003) The ubiquitin ligase activity in the DDB2 and CSA complexes is differentially regulated by the COP9 signalosome in response to DNA damage. Cell 113(3):357–367

Hardy RR, Carmack CE, Shinton SA (1991) Resolution and characterization of pro-B and pre-pro-B cell stages in normal mouse bone marrow. J Exp Med 173:1212–1225

Kawauchi K, Araki K, Tobiume K, Tanaka N (2008) p53 regulates glucose metabolism through an IKK-NF-kappaB pathway and inhibits cell transformation. Nat Cell Biol 10:611–618

Lassila O, Lambris JD, Gisler RH (1989) A role for Lys-His-Gly-NH avian and murine B cell development. Cell Immunol 122:319–328

Leopold JA, Cap A, Scribner AW, Stanton RC, Loscalzo J (1989) Glucose-6-phosphate dehydrogenase deficiency promotes endothelial oxidant stress and decreases endothelial nitric oxide bioavailability. FASEB J 15(10):1771–1773

Li DY, Geng ZR, Zhu HF, Wang C, Miao DN, Chen PY (2011) Immunomodulatory activities of a new pentapeptide (Bursopentin) from the chicken bursa of Fabricius. Amino Acids 40:505–515

Li D, Xue M, Geng Z, Pu Y (2012) The suppressive effects of bursopentine (BP5) on oxidative stress and NF-κB activation in lipopolysaccharide-activated murine peritoneal macrophages. Cell Physiol Biochem 29:9–20

Lydyard PM, Grossi CE, Cooper MD (1976) Ontogeny of B cells in the chicken I. Sequential development of clonal diversity in the bursa. J Exp Med 144:79–97

Meiners SD, Heyken A, Weller A, Ludwig K, Stangl PM, Kloetzel Kruger E (2003) Inhibition of proteasome activity induces concerted expression of proteasome genes and de novo formation of mammalian proteasomes. J Biol Chem 278:21517–21525

Moore RW, Caldwell DY (2003) Effect of bursal anti-steroidogenic peptide and immunoglobulin G on neonatal chicken B-lymphocyte proliferation. Comp Biochem Physiol Part C Toxicol Pharmacol 134:291–302

Munday R (1989) Toxicity of thiols and disulphides: involvement of free radical species. Free Radicul Biol Med 7:659–673

Orlowski M, Wilk S (1996) Ubiquitin-independent proteolytic functions of the proteasome. Arch Biochem Biophys 415:1–5

Piñol-Roma S (1997) HnRNP proteins and the nuclear export of mRNA. Semin Cell Dev Biol 8(1):57–63

Qiu Y, Shen Y, Li X, Liu Q, Ma Z (2008) Polyclonal antibody to porcine p53 protein: a new tool for studying the p53 pathway in a porcine model. Biochem Biophys Res Commun 377(1):151–155

Ruprecht CR, Lanzavecchia A (2006) Toll-like receptor stimulation as a third signal required for activation of human naive B cells. Eur J Immunol 36:810–816

Sato H, Tamba M, Ishii T, Bannai S (1999) Cloning and expression of a plasma membrane cystine-glutamate exchange transporter composed of two distinct proteins. J Biol Chem 274(17):11455–11458

Singh VK, Biswas S, Mathur KB, Haq W, Garg SK, Agarwal SS (1998) Thymopentin and splenopentin as immunomodulators. Immunol Res 17:345–368

Sundal E (1992) Thymopentin in cancer. Curr Ther Res 51:906–924

Takabe W, Kodama T, Hamakubo T, Tanaka K, Suzuki T, Aburatani H, Matsukawa N, Noguchi N (2001) Anti-atherogenic antioxidants regulate the expression and function of proteasome alpha-type subunits in human endothelial cells. J Biol Chem 276: 40497–40501

Tassi S, Carta S, Vené R, Delfino L, Ciriolo MR, Rubartelli A (2009) Pathogen-induced interleukin-1beta processing and secretion is regulated by a biphasic redox response. J Immunol 183: 1456–1462

Taylor SS, Ha E, McKeon F (1998) The human homologue of Bub3 is required for kinetochore localization of Bub1 and a Mad3/Bub1-related protein kinase. J Cell Biol 142(1):1–11

Thomas PJ, Garboczi DN, Pedersen PL (1992) Mutational analysis of the consensus nucleotide binding sequences in the rat liver mitochondrial ATP synthase b-subunit. J Biol Chem 267: 20331–20338

Yoo JY, Desiderio S (2003) Innate and acquired immunity intersect in a global view of the acute-phase response. Proc Natl Acad Sci 100:1157–1162

Yotov WV, StArnaud R (1993) Cloning and functional expression analysis of the alpha subunit of mouse ATP synthase. Biochem Biophys Res Commun 191:142–148